

Cluster-Induced Reactions at a Metal-Semiconductor Interface: Ce on Si(111)

M. Grioni, J. Joyce,^(a) S. A. Chambers,^(b) D. G. O'Neill,^(a) M. del Giudice, and J. H. Weaver
Department of Chemical Engineering and Materials Science, University of Minnesota, Minneapolis, Minnesota 55455
 (Received 27 August 1984)

Synchrotron-radiation photoemission, angle-resolved Auger, and LEED studies show Ce cluster formation on Si(111). These nonmetallic clusters grow for coverages of 0.1 to 0.6 monolayer, interact weakly with the substrate, and induce 200-meV band-bending changes. At ~ 0.6 monolayer, they stimulate surface disruption, producing a metallic interfacial silicide. The association of *d*- or *f*-band metal clusters with surface reaction substantially extends the cluster-induced-reaction model proposed for Al-GaAs.

PACS numbers: 73.30.+y, 73.40.Ns, 79.60.Gs

Microscopic examinations of evolving metal-semiconductor interfaces have revealed several systems that react only when the metal coverage, θ , exceeds a critical coverage, θ_c .¹⁻¹⁰ Modeling of these interfaces requires an understanding of the triggering phenomenon. Despite considerable efforts, however, the mechanism remains elusive.

Zunger¹¹ has suggested that cluster formation can induce defects at the Al-GaAs(110) interface. His total-energy calculations stressed adatom-adatom interaction through clustering, a point of view which differs from those which stress metal-substrate bonding.¹²⁻¹⁵ In light of the significance of this cluster mechanism, we sought a metal-semiconductor system in which the onset of chemical reaction could be linked to the evolution of clusters.

In this paper, we describe the room-temperature evolution of Ce clusters on Si(111)- 2×1 and -7×7 surfaces. High-resolution synchrotron-radiation photoemission, angle-resolved Auger spectroscopy,¹⁶ and LEED measurements show changes in both electronic structure and morphology. Indeed, this combination of techniques should make it possible to assess cluster formation for other interfaces and should reveal the relative importance of adatom-substrate and adatom-adatom bonding.

The photoemission experiments were performed at the Wisconsin Synchrotron Radiation Center using the "grasshopper" and toroidal grating monochromators for $12 \leq h\nu \leq 135$ eV. Photoelectrons were analyzed by a double-pass cylindrical-mirror analyzer with overall energy resolution of between 200 meV ($h\nu = 40$ eV) and 500 meV (135 eV). The angle-resolved Auger spectroscopy studies used a single-pass cylindrical-mirror analyzer with limited electron acceptance and a precision manipulator to vary the takeoff angle from normal emission to grazing emission. This detector was also used to obtain *I-V* LEED profiles along high-symmetry lines.

Clean Si(111)- 2×1 and -7×7 surfaces were produced by cleavage or standard Ar⁺ sputtering and annealing. High-purity cerium was evaporated at pressures better than 1×10^{-10} Torr; the thickness was monitored by an oscillating quartz crystal and the evaporation rate was ~ 1 Å/min [1 monolayer (ML) = 7.8×10^{14} atoms/cm² = 2.6 Å]. Operating pressures in both spectrometers were (3-5) $\times 10^{-11}$ Torr.

To demonstrate the existence of a critical coverage corresponding to the onset of reaction, we show in Fig. 1 Si 2*p* core-level spectra taken at $h\nu = 135$ eV (escape depth ~ 4 Å).¹⁷ For clean Si(111)- 2×1 , the 2*p* doublet is broadened by the surface-shifted component.¹⁷ Between zero and ~ 0.6 ML, there is a rigid shift of 200 meV due to variations in band bending (as confirmed by bulk-sensitive spectra at $h\nu = 106$ eV), but the unvarying line shape indicates minimal Ce-substrate interaction. Analysis of the Si-2*p* line shape for $\theta \geq 0.6$ ML reveals a reacted Si species shifted 0.7 eV to lower binding energy. This component grows and is most pronounced near 3 ML and the substrate component attenuates rapidly (discussed elsewhere using integrated intensities of the different components¹⁸). From coverage studies with 0.06-ML increments between 0 and 1 ML, we conclude that $\theta_c \approx 0.6$ ML.

LEED studies showed conversion from 2×1 or 7×7 patterns to 1×1 by ~ 0.4 ML but showed no metal-induced superstructure. The Si 1×1 pattern persisted through θ_c , although with increasing background. For 0.8 ML, where photoemission showed intermixing, LEED showed sufficient uncovered/unreacted Si for coherent diffraction (1×1 pattern). This indicates that the reaction could not be proceeding uniformly on the surface, and points to cluster-induced reaction. Even at 1.2 ML a 1×1 pattern, which was scarcely visible to the eye, could be detected by taking *I-V* measurements in high-symmetry azimuthal planes perpendicular to the

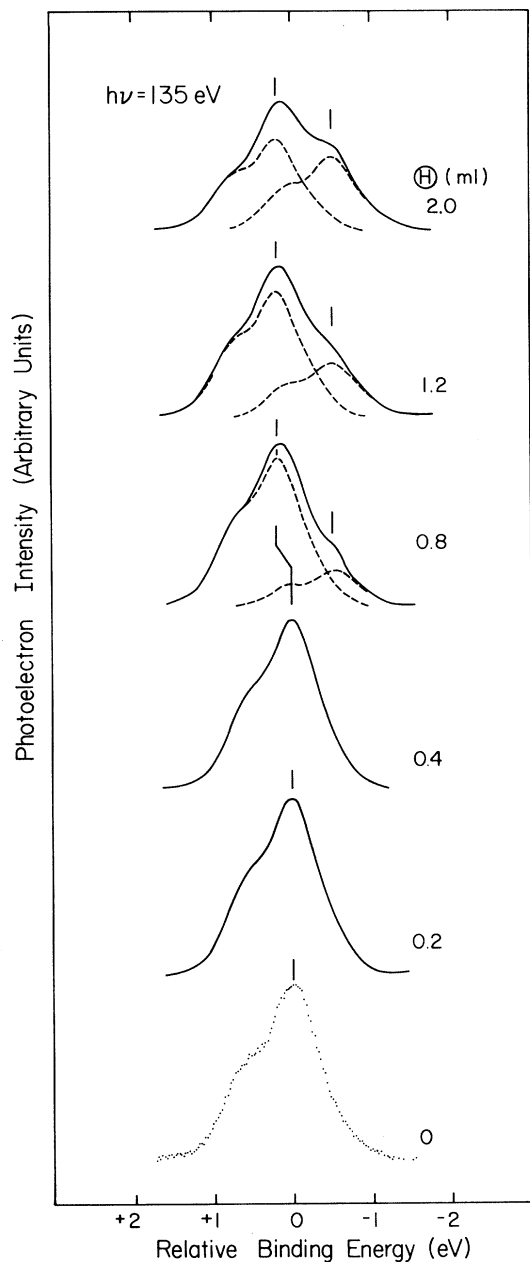


FIG. 1. Si $2p$ core total emission and deconvolution for cleaved Si(111)- 2×1 . The broken vertical line denotes the 200-meV change in band bending. Representative statistics are given by the dots for the clean surface at the bottom.

surface. By 2 ML, the (10), (11), and (20) LEED beams were completely gone, indicating the total destruction of long-range order. [Results concerning the annealed Ca-Si(111) interface will be presented elsewhere. A preliminary LEED investigation showed a high-temperature transition to an ordered ($\sqrt{3}\times\sqrt{3}$) phase.]

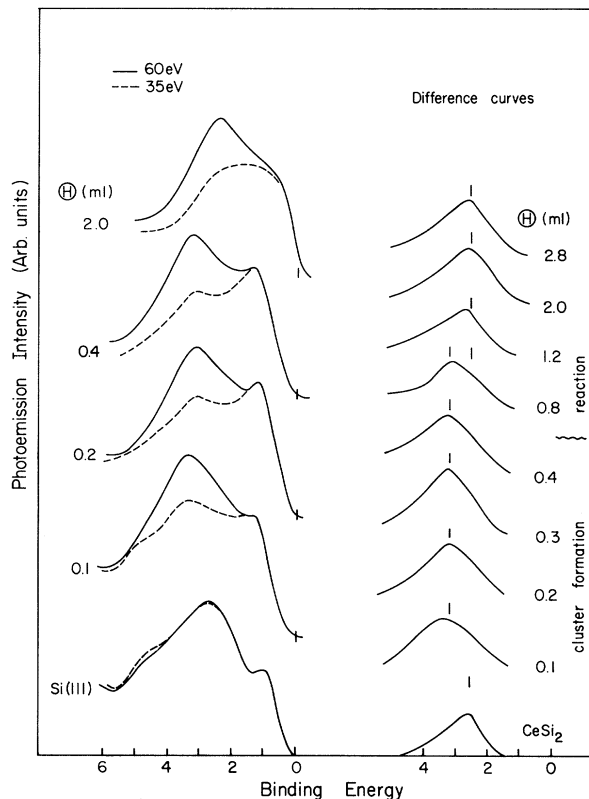


FIG. 2. Energy distribution curves for $h\nu = 35$ and 60 eV (left-hand side) and the difference curves (right-hand side) to highlight the Ce $4f$ character. Below 0.6 ML, the $4f$ indicates cluster formation. Above 0.6 ML, the $4f$ features shifts 0.7 eV and reflects local coordination with Si, as shown by comparison with CeSi_2 (bottom).

Valence-band studies at $h\nu = 35$ and 60 eV were undertaken to examine the electronic states at low coverage. Changes induced by d -derived states were readily seen at 35 eV; comparison of results for $h\nu = 35$ and 60 eV showed the emergence of Ce $4f$ emission.^{19,20} As shown in Fig. 2, the Ce-derived emission at -3.3 and -1.2 eV for $0.1 \leq \theta \leq 0.6$ ML rapidly overwhelms Si emission and, with increasing coverage, the feature at -1.2 eV grows in relative intensity. Simultaneously, the full width at half maximum (FWHM) measured at $h\nu = 35$ eV diminishes from ~ 4.4 eV for $\theta = 0.2$ ML to 3.9 eV for $\theta = 0.4$ ML. Consistent with the core-level results, we find that at $\theta \approx 0.6$ ML the valence-band center shifts abruptly toward E_F by ~ 0.7 eV and broadens sufficiently to lose its prominent doublet character. The appearance of the Fermi-level cutoff indicates metallic character for the reacted phase.

The valence-band results indicate cluster formation and growth for coverages 0 – 0.6 ML. Adatom-

induced states are clearly visible but are shifted away from E_F , analogously to what has been observed in all photoemission studies of weakly interacting clusters on inert substrates.²¹ The observed cluster bandwidth, which is substantially greater than that of bulk Ce,¹⁹ suggests a large number of inequivalent atoms, as observed for metal clusters. The absence of a Fermi level for $\theta \approx 0.6$ ML indicates that the molecular cluster has not reached the metallic droplet limit.

Studies of Ce $4f$ emission probe the environment around the Ce atom as effectively as Si $2p$ emission reveals the Si environment. Modification of the Ce environment above θ_c can be seen through difference spectra obtained by subtracting valence-band energy distribution curves at 35 and 60 eV which were normalized on the emission leading edge near -1 eV (Fig. 2). This procedure emphasizes the $4f$ character, as shown for α -Ce, γ -Ce,¹⁹ and the Ce pnictides.²⁰ Even for Ce coverages of 0.1 ML, a clearly defined spectral feature can be associated with the Ce $4f$ at -3.3 eV. The changing $4f$ fingerprint can therefore be used to assess chemical reaction ($4f$ final-state screening will be discussed elsewhere).

Figure 2 shows that the $4f$ feature sharpens but does not shift with coverage below θ_c . At $\theta = 0.8$ ML its appearance is modified by a shoulder at 0.7-eV-lower binding energy, and by 1.2 ML the $4f$ feature has fully shifted to the lower-binding-energy position. Comparison with results obtained from a bulk sample of CeSi₂ shows a silicide formation.

At the top of Fig. 3 we show Ce(N_4VV) and Si($L_{2,3}VV$) integrated Auger peak intensities measured at normal emission as a function of coverage. With increasing coverage, the Ce signal steadily increases while the Si signal is attenuated significantly from 0 to 0.4 ML. Between 0.4 and 0.8 ML, corresponding to the transition through θ_c , the Si attenuation is reduced. This behavior, which deviates from that expected for either ordered overlayers or an intermixed phase, can be explained by initial Ce coverage of a fraction of the substrate, followed by an intermediate region, 0.4–0.8 ML, where two processes compete. Initially, cluster formation attenuates the substrate, but this is offset by Si intermixing once reaction starts. The reacted regions then spread laterally, consuming more of the surface and attenuating the Si emission.

Polar-angle profiles of the Ce and Si Auger intensities measured in the $(\bar{1}10)$ azimuthal plane are shown in the lower two sections of Fig. 3. Structure in these polar profiles would reflect electrons

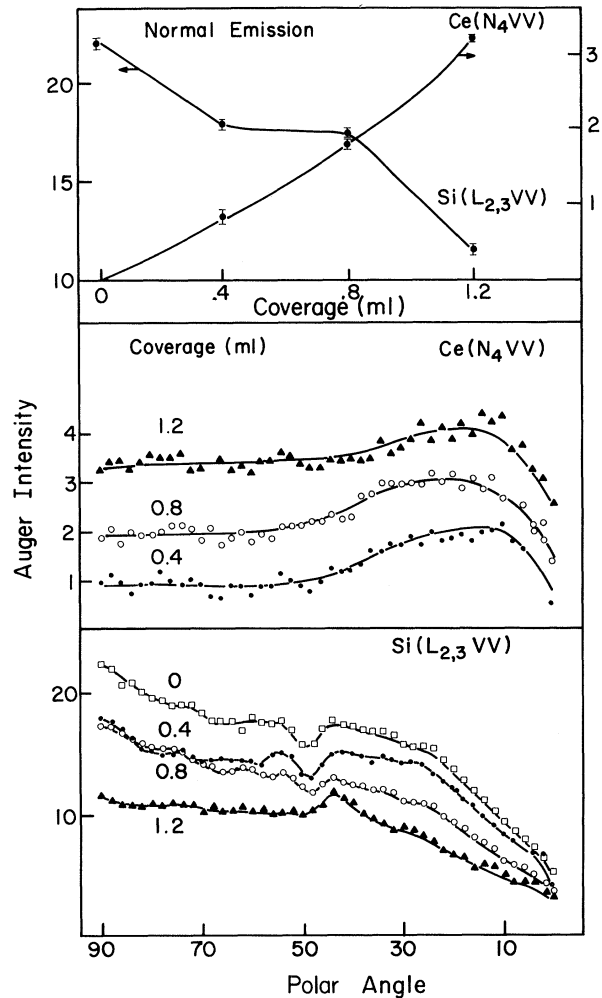


FIG. 3. Attenuation curves for Ce(N_4VV) and Si($L_{2,3}VV$) Auger intensity from normal-emission spectra for Si(111)(7×7) (top). Polar profiles are shown for the Ce(N_4VV) and Si($L_{2,3}VV$) Auger intensities for different coverages (middle and bottom). 90° is normal emission. All spectra are taken in the $(\bar{1}10)$ azimuthal plane perpendicular to the surface.

scattering from near-neighbor atoms and subsequent interference. For Ce, the results are featureless, consistent with disordered clusters. In contrast, the polar profile for clean Si shows diffraction modulation characteristic of the 7×7 surface, and this modulation remains in detail at 0.8 ML. Since atomic scattering factors for Ce are roughly three times those for Si for 100-eV electrons,²² a uniform Ce layer should obscure fine structure related to substrate emission. The persistence of substrate structure indicates that a substantial fraction of the Si electrons are unscattered, i.e., much of the surface is free of Ce. (Results for intermixed Au-Si show Si Auger diffraction fine structure to be

damped substantially more.) On the other hand, the Si attenuation reflects inelastic scattering of electrons which propagated through the Ce clusters. The damping of the fine structure at 1.2 ML indicates the increasing size of the reacted regions, consistent with cluster-induced reaction. By coverages of 4 ML, the Si polar profile is completely featureless.

We have shown here that clusters form by ~ 0.1 ML coverage, but produce Ce-Si intermixing only for $\theta \geq 0.6$ ML. Hence, the mechanism proposed by Zunger for Al-GaAs is not limited to simple metals on compound semiconductors, but may be important for a broad class of materials. We hope that this work will stimulate theoretical efforts to describe the early stages of interface formation, including clusters where appropriate, and establish the theoretical basis for the metal-overlayer-triggered reaction.

This work was supported by the U. S. Army Research Office under Contract No. DAAG29-83-K-0061 and a Northwest Area Foundation Grant of the Research Corporation. Discussions with G. Margaritondo, F. Grunthaner, and A. Franciosi are gratefully acknowledged.

^(a)Also at Materials Science Program, University of Wisconsin, Madison, Wisc. 53706.

^(b)Also at Department of Chemistry, Bethel College, St. Paul, Minn. 55112.

¹For an extensive review of metal-semiconductor interfaces see L. J. Brillson, *Surf. Sci. Rep.* **2**, 123 (1982).

²A. Franciosi, D. G. Peterman, J. H. Weaver, and V. L. Moruzzi, *Phys. Rev. B* **25**, 4981 (1982).

³J. H. Weaver, M. Grioni, and J. Joyce, to be published.

⁴A. Franciosi, P. Perfetti, A. D. Katnani, J. H. Weaver, and G. Margaritondo, *Phys. Rev. B* **29**, 5611 (1984).

⁵R. R. Daniels, A. D. Katnani, Te-Xiu Zhao, G. Margaritondo, and A. Zunger, *Phys. Rev. Lett.* **49**, 895 (1982).

⁶R. Ludeke and G. Landgren, *J. Vac. Sci. Technol.* **19**, 667 (1981).

⁷P. Skeath, I. Lindau, C. Y. Su, and W. E. Spicer, *Phys. Rev. B* **28**, 7051 (1983).

⁸J. Carelli and A. Kahn, *Surf. Sci.* **116**, 380 (1982).

⁹A. McKinley, G. J. Hughes, and R. H. Williams, *J. Phys. C* **15**, 7049 (1982).

¹⁰G. Rossi, J. Nogami, I. Lindau, L. Braicovich, I. Abbati, U. del Pennino, and S. Nannarone, *J. Vac. Sci. Technol.* **A1**, 781 (1983).

¹¹A. Zunger, *Phys. Rev. B* **24**, 4372 (1981).

¹²D. J. Chadi and R. Z. Bachrach, *J. Vac. Sci. Technol.* **16**, 1159 (1979).

¹³E. J. Mele and J. D. Joannopoulos, *Phys. Rev. Lett.* **42**, 1094 (1979).

¹⁴J. van Laar, H. Huijser, and T. L. van Rooy, *J. Vac. Sci. Technol.* **16**, 1164 (1979).

¹⁵S. E. Louie, J. R. Chelikowsky, and M. L. Cohen, *Phys. Rev. B* **15**, 2154 (1977).

¹⁶S. A. Chambers and L. W. Swanson, *Surf. Sci.* **131**, 385 (1983).

¹⁷F. J. Himpsel, P. Heimann, T.-C. Chiang, and D. E. Eastman, *Phys. Rev. Lett.* **45**, 1112 (1980).

¹⁸M. Grioni, J. Joyce, M. del Giudice, D. G. O'Neill, and J. H. Weaver, *Phys. Rev. B* (to be published).

¹⁹D. Wieliczka, J. H. Weaver, D. W. Lynch, and C. G. Olson, *Phys. Rev. B* **26**, 7056 (1982).

²⁰A. Franciosi, J. H. Weaver, N. Martensson, and M. Croft, *Phys. Rev. B* **24**, 3651 (1981).

²¹P. H. Citrin and G. K. Wertheim, *Phys. Rev. B* **27**, 3176 (1983), and detailed references therein.

²²M. Fink and A. C. Yates, *At. Data* **1**, 385 (1970).